

## ANTI-PROTON ANNIHILATION IN NUCLEI AS A PROBE OF QCD\*

Stanley J. Brodsky

Stanford Linear Accelerator Center  
Stanford University, Stanford, California 94309

Anti-proton annihilation in a nuclear target can test many novel aspects of quantum chromodynamics. In this talk I discuss a number of interesting features of such processes, including (1) the formation of nuclear-bound quarkonium, (2) tests of color transparency in hard, quasi-elastic nuclear reactions, (3) higher-twist, coherent, and formation zone effects in hard inclusive nuclear reactions, (4) reduced amplitude predictions for exclusive nuclear amplitudes, and (5) color filter effects in inclusive open and hidden charm production in nuclei.

## Introduction

Although quantum chromodynamics has been extensively tested in high momentum transfer reactions, the most challenging testing ground of the theory remains the detailed study of hadronic and nuclear phenomena at moderate energies and momentum transfer. We know that perturbative calculations in QCD must break down at momentum transfer of order  $\Lambda_{\overline{MS}}$ , the invariant momentum scale where the QCD running coupling constant  $\alpha_s(Q^2)$  becomes large. A recent determination<sup>1</sup> at LEP gives the values for  $\Lambda_{\overline{MS}} = 216 \pm 85 \text{ MeV}$ . On the other hand, scaling laws characteristic of the underlying quark and gluon degrees of freedom and subprocesses, particularly the Bjorken scale invariance of electroproduction structure functions and the inverse power law fall-off of electromagnetic form factors, are clearly evident at momentum transfer of 1 GeV or even less. Thus critical tests of QCD—at the intersection of perturbative and non-perturbative physics where coherent effects and hadron substructure become manifest—require the study of reactions with momentum transfers of only a few GeV or less.

Anti-protons can play a special role in testing QCD in the intermediate energy domain, particularly in total annihilation channels where all of the valence quarks and valence anti-quarks of the initial system are forced to annihilate at distances of the order of the proton Compton scale,  $\sim 1/M_p$ . Important annihilation processes include exclusive production of two-body systems, inclusive production of lepton-pairs and photon-pairs, and open and closed charm production near threshold. My main emphasis in this talk will be the study of the annihilation of anti-protons in nuclear matter, using the nucleus as a filter to sort out competing QCD sub-processes

\* Work supported by the Department of Energy contract DE-AC03-76SF00515.

Invited talk presented at the 1st Biennial Conference  
on Low Energy Antiproton Physics,  
Stockholm, Sweden, July 2-6, 1990

and different aspects of the hadronic wavefunctions. The nucleus can also modify QCD hadronization processes in a number of novel ways. In a sense, the background nuclear field plays the role in QCD that external magnetic and electric fields provide in atomic physics, allowing one to modify and probe the basic parameters of fundamental interactions. I will only have space here to give a brief description of the novel phenomena predicted by QCD for anti-proton interactions in nuclei. A more detailed discussion of many of these topics is given in Refs. 2 and 3.

## 1. THE NUCLEUS AS A QCD FILTER IN ANTI-PROTON REACTIONS

There are a large number of ways in which a nuclear target can probe fundamental aspects of QCD. A primary concept is that of the "color filter": if the interactions of an incident hadron are controlled by gluon exchange, then the nucleus will be transparent to those fluctuations of the incident hadron wavefunction which have small transverse size. Such Fock components have a small color dipole moment and thus will interact weakly in the nucleus; conversely, Fock components of normal hadronic size will interact strongly and be absorbed during their passage through the nucleus.<sup>4</sup> For example, large momentum transfer quasi-exclusive reactions, are controlled in perturbative QCD by small color-singlet valence-quark Fock components of transverse size  $b_{\perp} \sim 1/Q$ ; thus initial-state and final-state corrections to these hard reactions are suppressed at large momentum transfer, and they can occur in a nucleus without initial or final state absorption of the interacting hadrons. Thus at large momentum transfer and energies, quasi-elastic exclusive reactions occur additively in the nuclear volume, unaffected by initial or final state multiple-scattering or absorption of the interacting hadrons. This remarkable phenomenon is called "color transparency."<sup>6</sup> Thus QCD predicts that the "transparency ratio of quasi-elastic annihilation of the anti-proton in the  $\bar{p}p \rightarrow \ell\bar{\ell}$  reaction will be additive in proton number in a nuclear target.<sup>7, 8</sup>

$$\frac{d\sigma}{dQ^2}(\bar{p}A \rightarrow \ell\bar{\ell}(A-1)) \rightarrow Z^2 \frac{d\sigma}{dQ^2}(p\bar{p} \rightarrow \ell\bar{\ell}) \quad (1)$$

for asymptotic  $Q^2$ . In contrast to the QCD color transparency prediction, the traditional (Glauber) theory of nuclear absorption predicts that quasi-elastic scattering occurs primarily on the front surface of the nucleus. The above ratio thus should be proportional to  $Z^{2/3}$ , i.e. the number of protons exposed on the nuclear surface.

Conditions for Color Transparency Color transparency is a striking prediction of perturbative QCD at high momentum transfers. There are two effects which set the kinematic scale where the effect should be evident. First, the hard scattering subprocess must occur at a sufficiently large momentum transfer so that only small transverse size wavefunction components  $\psi(x_i, b_{\perp} \sim 1/Q)$  with small color dipole moments dominate the reaction. Second, the state must remain small during its

transit through the nucleus. The expansion distance is controlled by the time in which the small Fock component mixes with other Fock components. By Lorentz invariance, the time scale  $\tau = 2E_{\bar{p}}/\Delta M^2$  grows linearly with the energy of the hadron in the nuclear rest frame, where  $\Delta M^2$  is the difference of invariant mass squared of the Fock components. Estimates for the expansion time are given in references 9, 10, and 11.

There are a number of important tests of color transparency and color filter that can be carried out with anti-proton beams of moderate energy.<sup>12</sup> Since total annihilation processes such as  $p\bar{p} \rightarrow \ell\bar{\ell}$  or  $p\bar{p} \rightarrow \gamma\gamma$  and  $p\bar{p} \rightarrow J/\psi$  automatically involve short distances, the first condition for color transparency should be satisfied. The study of the energy dependence of these processes inside nuclei (quasi-elastic reactions, integrated over Fermi-motion) can clarify the role of the expansion time scale  $\tau$ . A recent analysis by Jennings and Miller<sup>10</sup> shows that  $\tau = 2E_{\bar{p}}/\Delta M^2$  is controlled by the mass difference of states which are close in mass to that of the asymptotic hadronic state. Thus color transparency may well be visible in low energy anti-proton annihilation processes, including quasi-elastic  $p\bar{p} \rightarrow J/\psi$  annihilation in the nucleus.

The only existing test of color transparency is the measurement of quasi-elastic large angle  $pp$  scattering in nuclei at Brookhaven.<sup>8</sup> The transparency ratio is observed to increase as the momentum transfer increases, in agreement with the color transparency prediction. However, in contradiction to perturbative QCD expectations, the data suggests, surprisingly, that normal Glauber absorption seems to recur at the highest energies of the experiment  $P_{lab} \sim 12 \text{ GeV}/c$ . It should be noted that this is the same kinematic domain where a strong spin correlation  $A_{NN}$  is observed.<sup>13</sup> The probability of protons scattering with their spins parallel and normal to the scattering plane is found to be twice that of anti-parallel scattering, which is again in strong contradiction to QCD expectations. However, Guy De Teramond and I<sup>14</sup> have noted that the breakdown of color transparency and the onset of strong spin-spin correlations can both be explained by the fact that the charm threshold occurs in  $pp$  collisions at  $\sqrt{s} \sim 5 \text{ GeV}$  or  $P_{lab} \sim 12 \text{ GeV}/c$ . At this energy the charm quarks are produced at rest in the center of mass. Since all of the eight quarks have zero relative velocity, they can resonate to give a strong threshold effect in the  $J = L = S = 1$  partial wave. (The orbital angular momentum of the  $pp$  state must be odd since the charm and anti-charm quarks have opposite parity.) This partial wave predicts maximal spin correlation in  $A_{NN}$ . Most important, such a threshold or resonant effect couples to hadrons of conventional size which will have normal absorption in the nucleus. If this non-perturbative  $pp \rightarrow pp$  amplitude dominates over the perturbative QCD amplitude, one can explain both the large spin correlation and the breakdown of color transparency at the charm threshold. Thus the nucleus acts as a filter, absorbing the non-perturbative contribution to elastic  $pp$  scattering, while allowing the hard scattering perturbative QCD processes to occur additively throughout the nuclear volume.<sup>15</sup> Similarly, one expects that the charm threshold will modify the color transparency and hard-scattering behavior of quasi-elastic  $p\bar{p}$  reactions in nuclei at

energies  $\sqrt{s} \sim 3 \text{ GeV}$ .

Diffraction Production of Jets in Anti-Proton Nuclear Reactions. In our original paper on the color filter, Bertsch, Goldhaber, Gunion, and I<sup>4</sup> suggested that diffractive nuclear reactions could be used as a color filter, i.e. fluctuations of an incident hadron with small color dipole moments and hence could emerge unscathed after transit through a nucleus without nuclear excitation. In the case of anti-proton reactions, the fluctuations of the valence Fock state where the three anti-quarks has small transverse separation and thus small color dipole moment will be produced in the form of three jets on the back side of the nucleus. The longitudinal and transverse momentum dependence of the  $p\bar{p}A \rightarrow A \text{ Jet Jet Jet}$  cross section will reflect the  $q\bar{q}q$  composition of the incident anti-proton wavefunction.

The Color Filter and Hadron Fragmentation in Nuclei. Recently, Hoyer and I<sup>16</sup> have shown that the color filter ansatz can explain the empirical rule that the nuclear dependence of hadronic spectra  $\frac{d\sigma/dx_F(HA-H'X)}{d\sigma/dx_F(HN-H'X)} = A^{\sigma(x_F)}$ , is nearly independent of particle type  $H'$ . The essential point is that fluctuations of the initial hadron  $H$  which have the small transverse size have the least differential energy loss in the nucleus. Anti-proton reactions can provide further tests of this explanation.

Color Transparency and Intrinsic Charm. A remarkable feature of the hadronic production of the  $J/\psi$  by protons in nuclei<sup>17,18</sup> is the fact that the cross section persists to high  $x_F$ , but with a strongly suppressed nuclear dependence,  $A^{\sigma(x_F)} \sim 0.7$ . The magnitude of the cross sections for high momentum charmonium reported by the NA-3 group<sup>17</sup> at CERN is, in fact, far in excess of what is predicted from gluon fusion or quark anti-quark annihilation subprocesses. Both the anomalous  $A$ -dependence and the high- $x_F$  excess can be explained by assuming the presence of intrinsic charm components of the incident hadron wave-functions.<sup>16</sup> The essential physics point is as follows: the intrinsic charm Fock components, e.g.  $|uudc\bar{c}\rangle$  in the proton have maximum probability when all of the quarks have equal velocities, i.e. when  $x_i \propto \sqrt{m^2 + k_{T,i}^2}$ . This implies that the charm and anti-charm quarks have the majority of the momentum of the proton when they are present in the hadron wavefunction. In a high energy proton-nucleus collision, the small transverse size, high- $x$  intrinsic  $c\bar{c}$  system can penetrate the nucleus, with minimal absorption and can coalesce to produce a charmonium state at large  $x_F$ . The remaining spectators of the nucleon have normal transverse size and interact on the front surface of the nucleus, leading to a production cross section approximately proportional to  $A^{0.7}$ . Since the formation of the charmonium state occurs far outside the nucleus at high energies, one predicts similar  $A^{\sigma(x_F)}$ -dependence of the  $J/\psi$  and  $\psi'$  cross sections, in agreement with recent results reported by the E772 experiment at Fermilab.<sup>18</sup> It would be very interesting to test these ideas using incident anti-protons over a wide range of beam momenta, since the fusion processes can be computed reliably in  $p\bar{p}$  inclusive reactions.

Shadowing, Anti-Shadowing of Inclusive Anti-Proton Reactions In the case of inclusive reactions, such as Drell-Yan massive lepton pair production  $\bar{p}p \rightarrow \ell\bar{\ell}X$ , multiple scattering of the interacting partons in the nucleus can lead to shadowing and anti-shadowing of the nuclear structure functions and a shift of the pair's transverse momentum to large transverse momentum. Hung Jung Lu and I have shown that nuclear shadowing of leading-twist QCD reactions can be related to Pomeron exchange in the multiple interactions of the quark or anti-quark in the nucleus, and that the complex phase of the quark-nucleon scattering amplitude due to non-singlet Reggeon exchange leads to anti-shadowing; i.e. an excess of the nuclear cross section over nucleon additivity.<sup>19</sup> It would be useful to probe in  $\bar{p}A$  reactions since there are almost no uncertainties in the knowledge of the incident parton distributions.

The definiteness of the leading order QCD predictions for  $\bar{p}p \rightarrow \ell\bar{\ell}$  reactions also makes the Drell Yan process an ideal reaction for isolating QCD dynamical higher twist processes. Power-law suppressed contributions must be present at some level of normalization due to the coherent annihilation of multi-quark systems. This includes correlated processes such as virtual meson annihilation and diquark annihilation  $\bar{q}q \rightarrow \ell\bar{\ell}$ . Since the diquark (correlated  $qq$ ) carries a high fraction of the proton's light-cone momentum fraction, such subprocesses give cross sections which can dominate leading twist contributions at  $x \sim 1$ . A representative form for the coherent contributions to the Drell-Yan reaction, including factors with the characteristic QCD end-point behavior at  $x \sim 1$  is:

$$\begin{aligned} \frac{d\sigma(\bar{p}p \rightarrow \ell\bar{\ell})}{d\Omega dx_1 dx_2} &= \frac{A(1-x_1)^3(1-x_2)^3(1+\cos^2\theta)}{Q^2} + \frac{B(1-x_1)(1-x_2)\sin^2\theta}{Q^6} \\ &+ \frac{C}{Q^{10}} \frac{1}{(1-x_1)(1-x_2)(1+\cos^2\theta)}. \end{aligned} \quad (2)$$

Dimensional counting and spectator counting rules  $dN/dx \sim (1-x)^{2N_{\text{spectator}}-1}$  are used here to determine the end-point behavior. Some modification of these predictions can occur because of spin selection rules. The lepton angular distribution reflects the coherence of the annihilating partons: e.g.  $\sin^2\theta$  for diquark-anti-diquark annihilation. The study of anti-proton annihilation into lepton pairs from low to high energies would allow the study of the transition of QCD mechanisms from full coherence to leading-twist incoherence.

There is empirical evidence for higher-twist contributions in the Drell-Yan due to the coherent  $\pi q \rightarrow \gamma^* \bar{q}$  subprocess. Measurements of the cross section for  $\pi N \rightarrow \mu^+ \mu^- X$  at CERN<sup>20</sup> are consistent with the prediction that the lepton angular distribution changes from  $1 + \cos^2\theta$  to  $\sin^2\theta$  at large  $x_F$  as the higher twist contribution becomes dominant.<sup>21</sup> Recently Qiu and Sterman<sup>22</sup> have extended the QCD fac-

torization theorem for general inclusive reactions to include next-to-leading-twist contributions of this type.

Formation Zone Effects in Anti-Proton Inclusive Reactions An essential aspect of the proofs of QCD factorization of inclusive reactions such as Drell-Yan massive lepton pair production in a nuclear target is that the entire nuclear dependence of the cross section is contained in the nuclear structure functions as measured in deep inelastic lepton-nucleus scattering. Thus the factorization theorem predicts that there is no initial state absorption or scattering that can significantly modify an incident hadron's parton distributions as it propagates through the nucleus. In particular, induced hard collinear radiation due to inelastic reactions in the nucleus before the annihilation or hard-scattering subprocess occurs must be dynamically suppressed. As shown by Bodwin, Lepage, and myself,<sup>23</sup> this suppression occurs automatically in the nucleus due to the destructive interference of the various multiple-scattering reactions in the nucleus. The interference occurs if the inelastic processes can occur coherently in the nucleus. This requires that the momentum transfer to target nucleons must be small compared to the inverse correlation length in the nucleus; i.e.  $E_q > \Delta M^2 L_A > 1$ , where  $E_q$  is the laboratory energy of the annihilating anti-quark,  $\Delta M^2$  is the change of mass squared of the quark in the inelastic reaction (small for hard collinear gluon emission of the anti-quark), and  $L_A$  is the length between target centers in the nucleus. It is important to test this formation zone effect by studying the nuclear dependence as a function of anti-quark laboratory energy in anti-proton reactions.

Exclusive Nuclear Amplitudes Exclusive nuclear reactions such as  $\bar{p}d \rightarrow \gamma n$  or  $\bar{p}d \rightarrow \pi^0 n$  can provide an important test of the reduced amplitude formalism for large momentum transfer exclusive nuclear reactions. Recent measurements at SLAC<sup>24</sup> are in striking agreement with the reduced amplitude predictions for photo-disintegration  $\gamma d \rightarrow np$  at a surprising low momentum transfer. The corresponding anti-proton reactions will allow an important test of both the scaling behavior of exclusive nuclear reactions and their crossing behavior to the annihilation channel. I will discuss this topic in more detail in Sections 3 and 4.

Hidden Color Nuclear Components In QCD the six-quark deuteron is a linear superposition of five color singlet states, only one of which corresponds to the conventional  $n-p$  state.<sup>25</sup> One can search for hidden color excitations of the deuteron in  $\bar{p}He^3$  elastic scattering at large angles.

Nuclear Bound Quarkonium The production of charmonium at threshold in a nuclear target is particularly interesting since it is possible that the attractive QCD van der Waals potential due to multi-gluon exchange could actually bind the  $\eta_c$  to light nuclei. Consider the reaction  $\bar{p}\alpha \rightarrow (\bar{c}c)H^3$  where the charmonium state is produced nearly at rest. At the threshold for charm production, the incident nuclei will be nearly stopped (in the center of mass frame) and will fuse into a compound nucleus because of the strong attractive nuclear force. The charmonium state will be attracted to the nucleus by the QCD gluonic van der Waals force. One thus expects strong

final state interactions near threshold. In fact, Guy De Teramond, Ivan Schmidt, and I<sup>26</sup> have argued that the  $c\bar{c}$  system will bind to the  $H^3$  nucleus. It is thus likely that a new type of exotic nuclear bound state will be formed: charmonium bound to nuclear matter.<sup>26</sup> Such a state should be observable at a distinct  $\bar{p}\alpha$  center of mass energy, spread by the width of the charmonium state, and it will decay to unique signatures such as  $\bar{p}\alpha \rightarrow H^3\gamma$ . The binding energy in the nucleus gives a measure of the charmonium's interactions with ordinary hadrons and nuclei; its hadronic decays will measure hadron-nucleus interactions and test color transparency starting from a unique initial state condition. I will discuss this topic in detail in the following section.

## 2. TESTING THE QCD VAN DER WAALS INTERACTION IN ANTI-PROTON INTERACTIONS<sup>26</sup>

In quantum chromodynamics, a heavy quarkonium  $Q\bar{Q}$  state such as the  $\eta_c$  interacts with a nucleon or nucleus through multiple gluon exchange. This is the QCD analogue of the attractive QED van der Waals potential. Unlike QED, the potential cannot have an inverse power-law at large distances because of the absence of zero mass gluonium states. Since the  $(Q\bar{Q})$  and nucleons have no quarks in common, the quark interchange (or equivalently the effective meson exchange) potential should be negligible. Since there is no Pauli blocking, the effective quarkonium-nuclear interaction will not have a short-range repulsion.

The QCD van der Waals interaction is the simplest example of a nuclear force in QCD.<sup>27</sup> In this paper we shall show that this potential is sufficiently strong to bind quarkonium states such as the  $\eta_c$  to nuclear matter. The signal for such states will be narrow peaks in energy in the production cross section. On general grounds one expects that the effective non-relativistic potential between heavy quarkonium and nucleons can be parameterized by a Yukawa form  $V(Q\bar{Q})_A = -\frac{g^2}{r}$ . Since the gluons have spin-one, the interaction is vector-like. This implies a rich spectrum of quarkonium-nucleus bound states with spin-orbit and spin-spin hyperfine splitting.

Thus far lattice gauge theory and other non-perturbative methods have not determined the range or magnitude of the gluonic potential between hadrons. A phenomenological estimate of the effective Yukawa potential applicable to mesonium bound states and resonances  $Q\bar{Q}Q$  has been given by Liu.<sup>28</sup> Using experimental evidence for resonant structure in both  $\phi - \phi$  and  $\psi - \psi$  systems, he finds an effective Yukawa potential for  $\phi - \psi$  interactions with strength  $\alpha \sim 0.45$  and inverse range  $\mu = 1 \text{ GeV}$ . One would expect the  $\eta_c - N$  interaction to have a somewhat larger magnitude and longer range.

We can obtain another estimate of the effective QCD Van der Waals potential using high energy information. Here we have in mind a QED analog, where one may use high energy lepton-lepton scattering to normalize the Coulomb potential at low energies. In our case, we relate vector-exchange contributions to the high energy

forward hadron-nucleon scattering amplitude to the vector part of the multi-gluon exchange potential at low energies. This should be a good approximation to the extent that the QCD Van der Waals potential behaves like a local spin one potential, analogous to vector boson exchange. In effect we identify pomeron exchange with the eikonalization of the two-gluon exchange potential.

We shall use the phenomenological model of high energy pomeron interactions developed by Donnachie and Landshoff<sup>29</sup>, where as in the Chou-Yang model, one has an  $s$ -independent parameterization of the meson-nucleon and meson-nucleus cross sections at small  $t$ :  $d\sigma/dt(MA \rightarrow MA) = [2\beta F_M(t)]^2 [3A\beta F_A(t)]^2 / 4s$ . Here  $\beta = 1.85 \text{ GeV}^{-1}$  is the flavor-independent pomeron-quark coupling constant, and  $A$  is the nucleon number of the nucleus. To first approximation the form factors can be identified with the helicity-zero meson and nuclear electromagnetic form factors.

Ignoring corrections due to eikonalization, the cross section at  $s \gg |t|$  can be identified with that due to the vector Yukawa potential  $d\sigma/dt(MA \rightarrow MA) = 4\pi\alpha^2 / (-t + \mu^2)^2$ . We then can calculate the effective coupling  $\alpha$  and the range  $\mu$  from  $(d\sigma/dt)^{1/2}$  and its slope at  $t = 0$ . For  $\pi - N$  or  $K - N$  scattering, one obtains  $\alpha \simeq 0.5$  and  $\mu \simeq 0.5 \text{ GeV}$ .

In the case of the  $\eta_c - N$  interaction, the radius of the meson is roughly half that of ordinary mesons.<sup>31</sup> In the fully-screened model of Guinon and Soper,<sup>32</sup> this reduces the total cross section by a factor of 4. In the Donnachie-Landshoff model,<sup>29</sup> screening is not so effective because of the approximately local coupling of the pomeron to hadrons. If we assume partial screening corresponding to a reduction of the elastic cross-section by a factor of two relative to  $K - N$  scattering,<sup>30</sup> we obtain  $\alpha = 0.4$  and  $\mu = 0.6 \text{ GeV}$  for the effective  $\eta_c - N$  potential. Non-screening corresponds to  $\alpha = 0.6$  and  $\mu = 0.6 \text{ GeV}$ . In either case these estimates are roughly consistent with Liu's values.

In the case of  $\eta_c$ -nucleus scattering, the slope is dominated by the nuclear size since the  $(c\bar{c})$  radius is comparatively small; thus  $\mu^{-2} = |dF_A(t)/dt|_{t=0} = \langle R_A^2 \rangle / 6$  and  $\alpha = 3A\beta^2\mu^2/2\pi$ , for the unscreened case. For  $\eta_c - He^3$  scattering, one finds  $\alpha \simeq 0.3$  and the inverse range is  $\mu \simeq 250 \text{ MeV}$  reflecting the smearing of the local interaction over the nuclear volume. For partially screened charmonium interactions,  $\alpha$  is reduced by  $1/\sqrt{2}$ . The QCD van der Waals potential is effectively the only QCD interaction between the charmonium bound state and nuclear matter. In the threshold regime the  $\eta_c$  is non-relativistic, and an effective-potential Schrödinger equation of motion is applicable. To first approximation we will treat the  $\eta_c$  as a stable particle. The effective potential is then real since higher energy intermediate states from charmonium or nuclear excitations should not be important.

The binding energy can be computed using the variational wavefunction  $\psi(r) = \sqrt{(\gamma^3/\pi)} \exp(-\gamma r)$ . Results for binding energies are presented in Table I for values of the coupling constant corresponding to the unscreened and partially screened cases. The condition for binding by the Yukawa potential with the above wavefunction

is  $\alpha m_{red} > \mu$ . This condition is not met for charmonium-proton or charmonium-deuteron systems. However, the binding of the  $\eta_c$  to a heavy nucleus increases rapidly with  $A$ , since the potential strength is approximately linear in  $A$ , and the kinetic energy  $< \vec{p}^2 / 2m_{red} >$  decreases faster than the square of the nuclear size. If the width of the  $c\bar{c}$  is much smaller than its binding energy, the charmonium state lives sufficiently long that it can be considered stable for the purposes of calculating its binding to the nucleus. For  $\eta_c H^3$  and  $\alpha = 0.33$  the computed binding energy is  $19 \text{ MeV}$ , and for  $\eta_c H^4$  the binding energy is over  $140 \text{ MeV}$ . The predicted binding energies are large even though the QCD van der Waals potential is relatively weak compared to the one-pion-exchange Yukawa potential; this is due to the absence of Pauli blocking or a repulsive short-range potential for heavy quarks in the nucleus. Table I gives a list of computed binding energies for the  $c\bar{c}$  nuclear systems. A two-parameter variational wavefunction of the form  $(e^{-\alpha_1 r} - e^{-\alpha_2 r})/r$  gives essentially the same results. Our results also have implications for the binding of hidden strange hadrons to nuclei.<sup>33</sup> However, the strong mixing of the  $\eta$  with non-strange quarks makes the interpretation of such states more complicated.

Table I

Binding energies  $\epsilon = | < H > |$  of the  $\eta_c$  to various nuclei, for unscreened and partially screened potentials; all masses are given in  $\text{GeV}$ . The data for  $< R_A^2 >^{1/2}$  (in  $\text{GeV}^{-1}$ ) are from ref. 34.

$A$	$< R_A^2 >^{1/2}$	$\mu$	$m_{red}$	unscreened		partially screened	
				$\alpha$	$\gamma$	$\alpha$	$\gamma$
1	3.9	0.60	0.715	0.59	$> 0$	0.42	$> 0$
2	10.7	0.23	1.15	0.172	$> 0$	0.122	$> 0$
3	9.5	0.26	1.45	0.327	0.40	0.231	0.24
4	8.2	0.30	1.66	0.585	0.92	0.414	0.62
6	11.2	0.22	1.95	0.470	0.89	0.332	0.61
					-0.128		-0.050

Searching for  $c\bar{c}$  Nuclear-Bound States It is clear that the production cross section for charm production near threshold in nuclei will be very small. However the signals for bound  $c\bar{c}$  to nuclei are very distinct. The most practical measurement could be the inclusive process  $p\bar{d} \rightarrow H^3 X$ , or  $\bar{p}\alpha \rightarrow H^3 X$ , where the missing mass  $M_X$  is constrained close to the charmonium mass. (See Fig. 1.) Since the decay of the bound  $c\bar{c}$  is isotropic in the center-of-mass, but backgrounds are peaked forward, the most favorable signal-to-noise is at backward  $H^3$  or  $H^4$  cm angles. If the  $\eta_c$  is bound to the recoil nucleus, a peak will be found at a distinct value of incident energy:  $\sqrt{s} = M_{\eta_c} + M_{H^3} - \epsilon$ , spread by the intrinsic width of the  $\eta_c$ . Here  $\epsilon$  is the  $\eta_c$ -nucleus binding energy predicted from the Schrödinger equation.

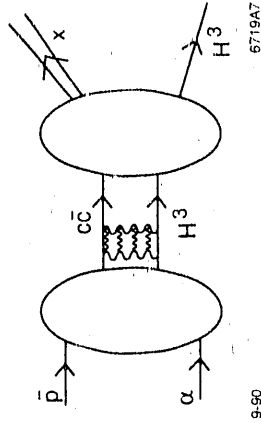


Figure 1. Formation of the  $(c\bar{c}) - H^3$  bound state in the process  $\bar{p}\alpha \rightarrow H^3 X$ .

The momentum distribution of the outgoing nucleus in the center-of-mass frame is given by  $dN/d^3p = |\psi(\vec{p})|^2$ . Thus the momentum distribution gives a direct measure of the  $c\bar{c}$ -nuclear wavefunction. The width of the momentum distribution is given by the wavefunction parameter  $\gamma$ , which is tabulated in Table I. The kinematics for several different reactions are given in Table II. From the uncertainty principle we expect that the final state momentum  $\vec{p}$  is related inversely to the uncertainty in the  $c\bar{c}$  position when it decays. By measuring the binding energy and recoil momentum distribution in  $\vec{p}$ , one determines the Schrödinger wavefunction, which then can be easily inverted to give the quarkonium-nuclear potential.

Energy conservation in the center of mass implies

$$E_{cm} = E_X + E_A \simeq M_X + M_A + \frac{\vec{p}^2}{2M_A'} \quad (3)$$

Here  $M_A' = (1/M_X + 1/M_A)^{-1}$  is the reduced mass of the final state system. The missing invariant mass is always less than the mass of the free  $\eta_c$ :

$$M_X = M_{\eta_c} - \epsilon - \frac{\vec{p}^2}{2M_A'} \quad (4)$$

Table II

Kinematics for the production of  $\eta_c$ -nucleus bound states. All quantities are given in GeV.

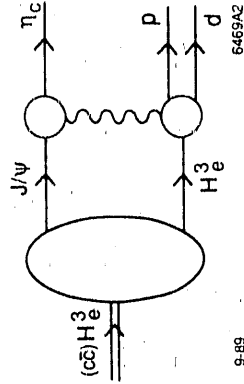
Process	$M_1$	$M_2$	$M_A$	$\epsilon$	$\sqrt{s}$	$p_{cm}$	$p_{lab}^*$
$\gamma He^3 \rightarrow (He^3 \eta_c)$	0	2.808	2.808	0.020	5.77	2.20	4.52
$pd \rightarrow (He^3 \eta_c)$	0.938	1.876	2.808	0.020	5.77	2.48	7.64
$\bar{p} He^4 \rightarrow (He^3 \eta_c)$	0.938	3.728	2.808	0.020	5.77	1.48	2.30
$\gamma He^4 \rightarrow (He^4 \eta_c)$	0	3.728	3.728	0.120	6.59	2.24	3.96
$n He^3 \rightarrow (He^4 \eta_c)$	0.938	2.808	3.728	0.120	6.59	2.60	6.09
$dd \rightarrow (He^4 \eta_c)$	1.876	1.876	3.728	0.120	6.59	2.71	9.51

thus the invariant mass varies with the recoil momentum. The mass deficit can be understood as the result of the fact that the  $\eta_c$  decays off its energy shell when bound to the nucleus.

More information is obtained by studying completely specified final states—exclusive channels such as  $\bar{p}\alpha \rightarrow \gamma\gamma H^3$ . Observation of the two-photon decay of the  $\eta_c$  would be a decisive signal for nuclear-bound quarkonia. The position of the bound  $\bar{c}\bar{c}$  at the instant of its decay is distributed in the nuclear volume according to the eigen-wavefunction  $\psi(\vec{r})$ . Thus the hadronic decays of the  $\bar{c}\bar{c}$  system allows the study of the propagation of hadrons through the nucleus starting from a wave-packet centered on the nucleus, a novel initial condition. In each case, the initial state condition for the decay is specified by the Schrödinger wavefunction with specific orbital and spin quantum numbers. Consider, then, the decay  $\eta_c \rightarrow p\bar{p}$ . As the nucleons transit the nuclear medium, their outgoing wave will be modified by nuclear final state interactions. The differential between the energy and momentum spectrum of the emitted proton and anti-proton should be a sensitive measure of the hadronic amplitudes. More interesting is the fact that the nucleons are initially formed from the  $\bar{c}\bar{c} \rightarrow g\bar{g}$  decay amplitude. The size of the production region is of the order of the charm Compton length  $\ell \sim 1/m_c$ . The out-going proton and anti-proton thus interact in the nucleus as a small color singlet state before they are asymptotic hadron states. The distortion of the outgoing hadron momenta thus tests formation zone physics<sup>30</sup> and color transparency.

**Possibility of  $J/\psi$ -Nucleus Bound States** The interactions of the  $J/\psi$  and other excited states of charmonium in nuclear matter are more complicated than the  $\eta_c$  interaction because of the possibility of spin-exchange interactions which allow the  $\bar{c}\bar{c}$

system to couple to the  $\eta_c$ . This effect, illustrated in Fig. 2, adds inelasticity to the effective  $\bar{c}\bar{c}$  nuclear potential. In effect the bound  $J/\psi - He^3$  can decay to  $\eta_c$ ,  $d$ ,  $p$  and its width will change from tens of KeV to MeV. However if the  $J/\psi$ -nucleus binding is sufficiently strong, then the  $\eta_c$  plus nuclear continuum states may not be allowed kinematically, and the bound  $J/\psi$  could then retain its narrow width,  $\approx 70$  KeV. As seen in Table I this appears to be the case for the  $J/\psi - He^4$  system. An important signature for the bound vector charmonium state will be the exclusive  $\ell^+\ell^-$  plus nucleus final state.



6469A2

9-89

Figure 2. Decay of the  $J/\psi - He^3$  bound state into  $\eta_c pd$ .

The narrowness of the charmonium states implies that the charmonium-nucleus bound state is formed at a sharp distinct cm energy, spread by the total width  $\Gamma$  and the much smaller probability that it will decay back to the initial state. By duality the product of the cross-section peak times its width should be roughly a constant. Thus the narrowness of the resonant energy leads to a large multiple of the peak cross section, favoring experiments with good incident energy resolution.

The formation cross section is thus characterized by a series of narrow spikes corresponding to the binding of the various  $\bar{c}\bar{c}$  states. In principle there could be higher orbital or higher angular momentum bound state excitations of the quarkonium-nucleus system. In the case of  $J/\psi$  bound to spin-half nuclei, we predict a hyperfine separation of the  $L = 0$  ground state corresponding to states of total spin  $J = 3/2$  and  $J = 1/2$ . This separation will measure the gluonic magnetic moment of the nucleus and that of the  $J/\psi$ . Measurements of the binding energies could in principle be done with excellent precision, thus determining fundamental hadronic parameters with high accuracy.

**Stopping Factor** The production cross section for creating the quarkonium-nucleus bound state is suppressed by a dynamical "stopping" factor representing the probability that the nucleons and nuclei in the final state convert their kinetic energy to the heavy quark pair and are all brought to approximately zero relative velocity. For example, in the reaction  $pd \rightarrow (\bar{c}\bar{c})He^3$  the initial proton and deuteron must each change momentum from  $p_{cm}$  to zero momentum in the center of mass. The probability for a nucleon or nucleus to change momentum and stay intact is given by the

### 3. EXCLUSIVE ANTI-PROTON REACTIONS

A primary test of QCD in exclusive reactions<sup>5</sup> is the time-like Compton process:  $\bar{p}\bar{p} \rightarrow \gamma\gamma$ . Many features of this annihilation reaction can be predicted from first principles at large momentum transfer. The amplitude can be factorized in the form of a hard scattering amplitude  $T_H$  for the annihilation  $q\bar{q}q\bar{q}q\bar{q} \rightarrow \gamma\gamma$ , convoluted with the proton distribution amplitudes,  $\phi_p(x_i; Q)$ ,  $\phi_{\bar{p}}(x_i; Q)$ ,  $x_1 + x_2 + x_3 = 1$ , the basic amplitude that controls the distribution of light-cone momentum of the three quarks in the lowest particle (valence) wavefunction. at the momentum scale  $Q \sim pT$ . The nominal scaling law predicted from QCD and dimensional counting is

$$\frac{d\sigma}{dt}(\bar{p}\bar{p} \rightarrow \gamma\gamma) = \frac{\alpha^2 \alpha_s^2(pT) f(\cos \theta_{cm})}{s^6} \quad (6)$$

The angular dependence  $f(\cos \theta_{cm})$  reflects both the structure of the perturbative graphs that control  $T_H$  and the shapes of the distribution amplitude. Measurements of the Compton process  $\bar{p}\bar{p} \rightarrow \gamma\gamma$  is thus important for a number of reasons: (1) The  $s$  dependence at fixed  $\theta_{cm}$  checks the fundamental scaling law of the perturbative theory. (2) The shape of the angular dependence gives a measure of the distribution amplitude of the proton. (3) Comparison with measurements of the proton Compton amplitude allow one to test the crossing properties of the QCD predictions. (4) The helicity structure of the amplitudes reflects the underlying chiral invariance of the theory. The dominant contribution corresponds to hadron helicity conservation i.e.  $\lambda_p + \lambda_{\bar{p}} = 0$ . (5) The dominant amplitude at large transverse momentum should be approximately independent of photon mass; vector meson dominance contributions should be power-law suppressed. (6) The amplitude should obey color transparency; i.e. minimal absorption of the anti-proton when one measures quasi-elastic  $\bar{p}A \rightarrow \gamma\gamma(A-1)$  in a heavy nuclear target. As discussed in the introduction this violation of traditional nuclear physics absorption theory reflects the fact that the dominant amplitude at large transverse momentum is controlled by the fluctuation of the anti-proton wavefunction when it contains just the three anti-quarks at transverse separation  $b_{\perp} \sim 1/p_{\perp}$ . Such a wavefunction has a small color dipole moment and thus has minimal hadronic interactions in the nucleus.

Detailed predictions<sup>39</sup> for the process  $\bar{p}\bar{p} \rightarrow \gamma\gamma$  and the reversed reaction  $\gamma\gamma \rightarrow \bar{p}\bar{p}$  have been given for real and virtual photons by Farrar, *et al.* For definiteness one assumes the shape and normalization of the distribution amplitude given by QCD sum rule constraints. Existing measurements of  $\gamma\gamma \rightarrow \bar{p}\bar{p}$  in two-photon experiments are at too low of energy to test the leading twist predictions; however, the observed magnitude of the cross section at  $\approx 5 \text{ GeV}^2$  is of the correct size predicted by the theory.

The time-like Compton process is just one example of  $\bar{p}p$  annihilation exclusive processes important for testing QCD. The reactions include:

$$\bar{p}p \rightarrow e^+e^-, \gamma\gamma, \gamma M^0, M\bar{M}, M\bar{B}, B\bar{B} \quad (7)$$

square of its form factor  $F_A^2(q_A^2)$ , where  $q_A^2 = [(M_A^2 + p_{cm}^2)^{1/2} - M_A]^2 - p_{cm}^2$ . We can use as a reference cross section the  $pp \rightarrow c\bar{c}pp$  cross section above threshold, which was estimated in Ref. 14 to be of order  $\sim 1\mu\text{b}$ . Then

$$\sigma(A_1 A_2 \rightarrow c\bar{c} A_{12}) = \sigma(pp \rightarrow c\bar{c} pp) \frac{F_{A_1}^2(q_{A_1}^2) F_{A_2}^2(q_{A_2}^2)}{F_N^2(q_N^2)} \quad (5)$$

We thus obtain a suppression factor relative to the  $pp$  channel of  $F_A^2(4.6 \text{ GeV}^2) F_p^2(3.2 \text{ GeV}^2) / F_N^2(2.8 \text{ GeV}^2) \sim 10^{-5}$  for the  $p\bar{d} \rightarrow c\bar{c} H e^3$  channel, giving a cross section which may be as large as  $10^{-35} \text{ cm}^2$ . In the case of the  $\bar{p}\alpha$  reaction, one requires the annihilation of the anti-proton on a proton with high virtual momentum components: above threshold, one can write  $d\sigma(\bar{p}A \rightarrow \eta_c(A-1))/dx = G_{p/A}(x)\sigma(\bar{p}p \rightarrow \eta_c)$ . Information on the shape of the required quasi-exclusive  $A \rightarrow p(x)(A-1)$  fractional momentum distribution (essentially an inelastic form factor squared) for virtual protons in a nucleus can be obtained theoretically from spectator counting rules or experimentally by measuring the corresponding form factors in electroproduction or nuclear fragmentation experiments. Large enhancements of this rate would be expected near threshold. Considering the uniqueness of the signal and the extra enhancement at the resonance energy, it is likely that both the  $\bar{p}\alpha$  and  $p\bar{d}$  formation experiments are experimentally viable.<sup>36</sup>

Conclusions on Nuclear-Bound Quarkonium In QCD, the nuclear forces are identified with the residual strong color interactions due to quark interchange and multiple-gluon exchange.<sup>37</sup> Because of the identity of the quark constituents of nucleons, a short-range repulsive component is also present (Pauli-blocking). From this perspective, the study of heavy quarkonium interactions in nuclear matter is particularly interesting: due to the distinct flavors of the quarks involved in the quarkonium-nucleon interaction there is no quark exchange to first order in elastic processes, and thus no one-meson-exchange potential from which to build a standard nuclear potential. For the same reason, there is no Pauli-blocking and consequently no short-range nuclear repulsion. The nuclear interaction in this case is purely gluonic and thus of a different nature from the usual nuclear forces.

The production of nuclear-bound quarkonium would be the first realization of hadronic nuclei with exotic components bound by a purely gluonic potential. Furthermore, the charmonium-nucleon interaction would provide the dynamical basis for understanding the spin-spin correlation anomaly in high energy  $p-p$  elastic scattering.<sup>14</sup> In this case, the interaction is not strong enough to produce a bound state, but it can provide a strong enough enhancement at the heavy-quark threshold characteristic of an almost-bound system.<sup>38</sup>

In each case one can make detailed predictions based on factorization theorems, evolution equations for the logarithmic  $\log Q^2$  dependence of meson and baryon distribution amplitudes, scaling laws for the hard scattering distributions (dimensional counting rules). In most cases one has to analyze the Landshoff pinch singularity diagrams, which correspond to multiple quark scattering through the same angle. A recent careful analysis by Botts and Sterman has confirmed Mueller's explicit calculation of the Sudakov suppression of these singularities and their dominance by short distance distribution amplitudes. Thus up to small corrections, one predicts fixed-angle scaling:  $\frac{d\sigma}{dt} = \frac{f(\theta_{cm})}{s^{N-2}}$  where  $N = N_A + N_B + N_C + N_D$  is the total minimum number of elementary quark, lepton, or photon fields participating in the hard subprocess. In each case one predicts hadron helicity conservation:  $\lambda_A + \lambda_B = \lambda_C + \lambda_D$ , independent of the photon or lepton helicity. One can also test mechanisms for the hard scattering subprocess with simple crossing properties: e.g. the quark interchange amplitude for proton-proton scattering has the approximate form:  $\frac{d\sigma}{dt}(pp \rightarrow pp) \approx \frac{1}{s} \frac{1}{t} \frac{1}{u}$ . If this is the dominant mechanism for  $pp$  scattering then by  $s \leftrightarrow u$  crossing one predicts:  $\frac{d\sigma}{dt}(\bar{p}p \rightarrow \bar{p}p) \approx \frac{1}{s} \frac{1}{t}$ ; i.e. a forward, but no backward peak in  $\theta_{cm}$ .

#### 4. REDUCED NUCLEAR AMPLITUDES

Explicit signals of QCD in nuclei have been elusive, in part because of the fact that an effective Lagrangian containing meson and nucleon degrees of freedom must be in some sense equivalent to QCD if one is limited to low-energy probes. The distinction between QCD and other treatments of nuclear amplitudes is particularly clear in the reaction  $\gamma d \rightarrow n\bar{p}$ ; i.e. photodisintegration of the deuteron at fixed center of mass angle. Using dimensional counting, the leading power-law prediction from QCD is simply  $\frac{d\sigma}{dt}(\gamma d \rightarrow n\bar{p}) \sim F(\theta_{cm})/s^{11}$ . Of course in the nuclear amplitude, the virtual momenta are partitioned among many quarks and gluons, so that finite mass corrections will be significant at low to medium energies. Nevertheless, there is an elegant way to test the basic QCD dynamics in these reactions taking into account much of the finite-mass, higher-twist corrections by using the "reduced amplitude" formalism.<sup>40</sup> The basic observation is that for vanishing nuclear binding energy  $\epsilon_d \rightarrow 0$ , the deuteron can be regarded as two nucleons sharing the deuteron four-momentum (see Fig. 3). The momentum  $\ell$  is limited by the binding and can thus be neglected. Thus the photodisintegration amplitude contains the probability amplitude (i.e. nucleon form factors) for the proton and neutron to each remain intact after absorbing momentum transfers  $p_p - 1/2p_d$  and  $p_n - 1/2p_d$ , respectively. After the form factors are removed, the remaining "reduced" amplitude should scale as  $F(\theta_{cm})/\sqrt{t}$ . The single inverse power of transverse momentum  $\sqrt{t}$  is the slowest conceivable in any theory, but it is the unique power predicted by PQCD.

A test of the prediction that  $f(\theta_{cm})$  is energy dependent at high-momentum transfer is compared with experiment in Fig. 4. It is remarkable to see the QCD prediction verified at incident photon lab energies as low as 1 GeV. A comparison with a standard nuclear physics model with exchange currents is also shown for comparison

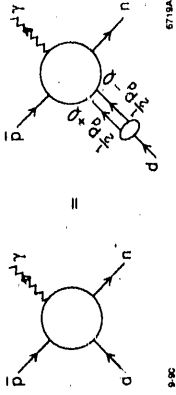


Figure 3. Construction of the reduced nuclear amplitude for the two-body inelastic deuteron reactions  $\bar{p}d \rightarrow \gamma n$ .

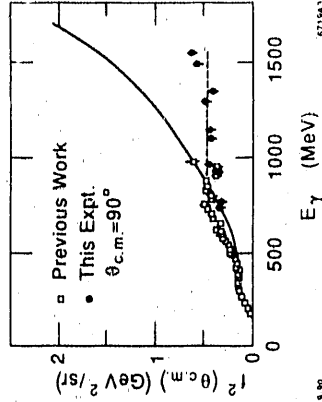


Figure 4. Comparison of deuteron photodisintegration data with the scaling prediction (dotted line) which requires  $f(\theta_{cm})$  to be at most logarithmically dependent on energy at large momentum transfer. The data are from the recent experiment of Ref. 24. The nuclear physics prediction (solid curve) is the meson-exchange current calculation of Ref. 42.

in Fig. 4. The fact that this prediction falls less fast than the data suggests that meson and nucleon compositeness are not taken into account correctly.

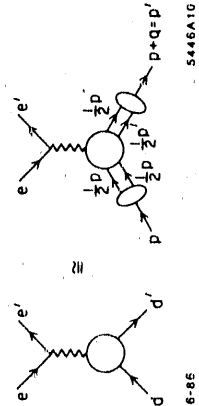
There are a number of related tests of QCD and reduced amplitudes which require  $\bar{p}$  beams,<sup>41</sup> including  $\bar{p}d \rightarrow \gamma n$  and  $\bar{p}d \rightarrow \pi^- p$  in the fixed  $\theta_{cm}$  region. Dimensional counting rules predict the asymptotic behavior  $\frac{d\sigma}{dt}(\bar{p}d \rightarrow \pi^- p) \sim f(\theta_{cm})/(s^2)^{12}$ , since there are 14 initial and final quanta involved. One cannot expect the onset of such scaling laws until  $\sqrt{t}$  is well into the multi-GeV regime since each hard propagator must carry significant momentum transfer. However, again one notes that the  $\bar{p}d \rightarrow \pi^- p$  amplitude contains a factor representing the probability amplitude (i.e. form factor) for the proton to remain intact after absorbing momentum transfer squared  $\hat{t} = (p - 1/2pd)^2$  and the  $\bar{N}N$  time-like form factor at  $\hat{s} = (\bar{p} + 1/2pd)^2$ . Thus  $M_{\bar{p}d \rightarrow \pi^- p} \sim F_{1N}(\hat{t}) F_{1N}(\hat{s}) M_r$ , where  $M_r$  has the same QCD scaling properties as quark meson scattering. We thus predict

$$\frac{d\sigma}{dt}(\bar{p}d \rightarrow \pi^- p) \frac{f(\Omega)}{F_{1N}^2(t) F_{1N}^2(s)} \sim \frac{f(\Omega)}{p_T^2} \quad (8)$$

The analogous analysis of the deuteron form factor as defined in

$$\frac{d\sigma}{dt}(ed \rightarrow ed) = \frac{d\sigma}{dt} \Big|_{\text{point}} (F_d(Q^2))^2 \quad (9)$$

yields a scaling law for the reduced form factor (see Fig. 5):



5446A10

6-86

Figure 5. Application of the reduced amplitude formalism to the deuteron form factor at large momentum transfer.

$$f_d(Q^2) \equiv \frac{F_d(Q^2)}{F_{1N}\left(\frac{Q^2}{4}\right) F_{1N}\left(\frac{Q^2}{4}\right)} \sim \frac{1}{Q^2} \quad (10)$$

i.e. the same scaling law as a meson form factor. As shown in Fig. 6, this scaling is consistent with experiment for  $Q = p_T \gtrsim 1$  GeV. We have also seen the evidence for reduced amplitude scaling for  $\gamma d \rightarrow pn$  at large angles and  $p_T \gtrsim 1$  GeV. (see Fig. 4). We thus expect similar precocious scaling behavior to hold for  $\bar{p}d \rightarrow \pi^- p$  and other  $\bar{p}d$  exclusive reduced amplitudes. All of these exclusive nuclear amplitudes provide important tests of the influence of scale-invariant quark-gluon interactions in the nuclear domain.

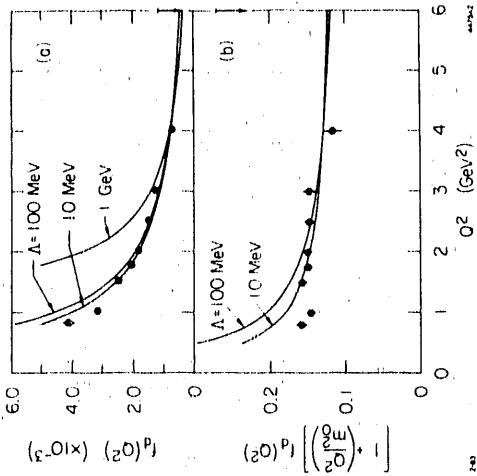


Figure 6. Scaling of the deuteron reduced form factor  $f_d(Q^2)$ . The QCD reduced amplitude analysis predicts  $Q^2 f_d(Q^2) \sim \text{constant}$  at large  $Q^2$ . The data are summarized in Ref. 40.

## 5. ACKNOWLEDGEMENTS

Some of the material presented here is based on collaborations with others, particularly G. de Teramond, J. R. Hiller, P. Hoyer, G. P. Lepage, H. J. Lu, A. H. Mueller, and I. Schmidt. I also wish to thank Per Carlson, Kerstin Jon-And, and their colleagues at the Manne Siegbahn Institute of Physics, for their outstanding hospitality in Stockholm and a very interesting conference.

## REFERENCES

1. M. Z. Akrawy et al. (OPAL collaboration) CERN-PPE/90-121, (1990)
2. S. J. Brodsky, SLAC-PUB-4749, published in the proceedings of the International School of Physics with Low Energy Anti-Protons, Erice (1988).
3. S. J. Brodsky, SLAC-PUB-5116, published in the proceedings of the 27th International School of Subnuclear Physics, Erice (1989).
4. G. Bertsch, S. J. Brodsky, A. S. Goldhaber, and J. Gunion, Phys. Rev. Lett. **47**, 297 (1981).
5. Exclusive processes in QCD are reviewed in S. J. Brodsky and G. P. Lepage, in *Quantum Chromodynamics*, edited by A. H. Mueller, (World Scientific, 1990.)
6. A. H. Mueller, Proc. XVII Rencontre de Moriond (1982); S. J. Brodsky, Proc. XIII International Symposium on Multiparticle Dynamics, Volendam (1982); S. J. Brodsky and A. H. Mueller, Phys. Lett. **206B**, 685 (1988). and references therein.
7. By definition, quasi-elastic processes are nearly coplanar, integrated over the Fermi motion of the protons in the nucleus. Such processes are nearly exclusive in the sense that no extra hadrons are allowed in the final state.
8. A. S. Carroll, et al., Phys. rev. Lett. **61**, 1698 (1988).
9. J. P. Ralston and B. Fire, Phys. Rev. Lett. **61**, 1823 (1988), University of Kansas preprint 90-0548 (1990).
10. B. K. Jennings and G. A. Miller, Phys. Lett. **B236**, 209 (1990). and University of Washington preprint (1990).
11. G. R. Farrar, H. Liu, L. L. Frankfurt, M. I. Satrikman, Phys. Rev. Lett. **61**, 686 (1988).
12. For additional discussion, see also, A. B. Kaidalov, presented at the LEAR Workshop (1990).
13. G. R. Court, et al., Phys. Rev. Lett. **57**, 507 (1986).
14. S. J. Brodsky and G. de Teramond, Phys. Rev. Lett. **60**, 1924 (1988).
15. For an alternative explanation, see ref. 9.
16. S. J. Brodsky and P. Hoyer, Phys. Rev. Lett. **63**, 1566 (1990); S. J. Brodsky, C. Peterson, and N. Sakai, Phys. Rev. **D23**, 2745 (1981). E. Hoffmann and R. Moore, Z. Phys. **C20**, 91 (1990). For a recent estimate of intrinsic charm matrix elements from OZI-violation in baryons, see T. Hatsuda and T. Kunihiro, CERN-TH. 5386 (1990).
17. J. Badier, et al, Z. Phys. **C20**, 101 (1983); P. Charpentier, Saclay Thesis CEA-N-237 (1984).
18. D. M. Alde, et. al., Phys. Rev. Lett. **64**, 2479 (1990), Los Alamos preprint LA-UR-90-2331 (1990), and references therein.
19. S. J. Brodsky and H. J. Lu, Phys. Rev. Lett. **64**, 1342 (1990).
20. S. Palestini, et al., Phys. Rev. Lett. **55**, 2649 (1985); C. Naudet et al., Phys. Rev. Lett. **56**, 808 (1986).
21. E. L. Berger and S. J. Brodsky, Phys. Rev. Lett. **42**, 940 (1979).
22. J.-W. Qiu and G. Sterman, ITP-SB-90-49/50, (1990).
23. G. T. Bodwin, S. J. Brodsky, and G. P. Lepage, Phys. Rev. **D39**, 3287 (1989).
24. J. Napolitano et al., Phys. Rev. Lett. **61**, 2530 (1988).
25. For a recent review on the status of di-baryon hidden color resonances, see E. Lomon, MIT preprint (1990).
26. S. J. Brodsky, G. de Teramond, and I. Schmidt, Phys. Rev. Lett. **64**, 1011 (1990).
27. Multiple gluon exchange is difficult to distinguish from effective  $\omega$  exchange. Nevertheless, in principle, the QCD van der Waals interaction provides an attractive vector-like isospin-zero potential which should be added to the usual meson-exchange potential; this may have implications for low energy nuclear physics studies, such as nucleon-nucleon scattering and binding.
28. K.-F. Liu, private communication; B.-A. Li and K.-F. Liu, Phys. Rev. **D29** 426 (1984).
29. A. Donnachie and P. V. Landshoff, Nucl. Phys. **B244**, 322 (1984). In order to account for the additive quark rule for total cross sections in this picture, the pomeron must have a somewhat local structure for momenta below the scale  $\mu_0 \sim 1 \text{ GeV}$ ; its couplings are analogous to that of a heavy photon. Interference terms involving different quarks at transverse separation  $b_T > 1/\mu_0 \sim 0.2 \text{ fm}$  which screen the color interactions can then be neglected.
30. At present there is no experimental constraint on the physical  $J/\psi - N$  cross section. The cross section deduced from the  $A$ -dependence of  $J/\psi$  photoproduction in nuclei underestimates the true charmonium-nucleon cross section since at high energies the  $J/\psi$  is formed outside the nucleus; see S. J. Brodsky and A. H. Mueller, ref. 6.
31. See, e.g., W. Kwong, J. L. Rosner and C. Quigg, Ann. Rev. Nucl. Part. Sci. **37**, 325 (1987). Note that the mean radius estimated in this work is the distance between the heavy quarks, which is roughly twice the RMS charmonium radius.
32. J. F. Gunion and D. E. Soper, Phys. Rev. **D15**, 2617 (1977).
33. R. E. Chrien et al., Phys. Rev. Lett. **60**, 2595 (1988), and refs. therein; J. L. Rosen, Northwestern University preprint (1988).
34. R. Hofstadter, Ann. Rev. of Nuclear Science **7**, 231 (1957). The  $He^3$  and  $He^4$  data are from J. S. McCarthy et al., Phys. Rev. **C15**, 1396 (1977).
35. D. B. Lichtenberg and J. G. Wills, Nuovo Cimento **47A**, 483 (1978).

36. A detailed design for an experimental search for nuclear-bound charmonium in anti-proton collisions has been given by K. Maruyama and S. Endo, University of Tokyo Preprint INS-REP-837 (Aug. 1990).
37. See, for example, S. A. Williams *et al.*, Phys. Rev. Lett. **49**, 771 (1982).
38. The signal for the production of almost-bound nucleon (or nuclear) charmonium systems near threshold is the isotropic production of the recoil nucleon (or nucleus) at large invariant mass  $M_X \simeq M_{\psi}$ ,  $M_{J/\psi}$ .
39. G. R. Farrar, E. Maina, F. Neri Nucl. Phys. **B259**, 702 (1985), **B263**, 746 (1986); see also J. F. Gunion, D. Millers, K. Sparks Phys. Rev. **D33**, 689 (1986).
40. S. J. Brodsky and B. T. Chertok, Phys. Rev. Lett. **37**, 269 (1976), Phys. Rev. **D114**, 3003 (1976); S. J. Brodsky and J. R. Hiller, Phys. Rev. **C28**, 475 (1983).
41. C. R. Ji and S. J. Brodsky, Phys. Rev. **D33**, 1951, 1406, 2653, (1986).
42. T. S.-H. Lee, ANL preprint (1988).
43. The data are compiled in Brodsky and Hiller, Ref. 40.

**END**

**DATE FILMED**

10 / 31 / 90